undergo programmed cell death because they do not fragment their DNA (*12*). Rather, antigen-stimulated $CD4^-CD8^{lo}$ precursor thymocytes may become $CD4^-CD8^-TCR\alpha\beta^+$ thymocytes, which would explain the disproportionate appearance of such thymocytes in Tg-TCRαβ male mice (*3*, *4*).

Our data show that TCR signals generated in $CD4^-CD8^{lo}$ precursor thymocytes can clonally regulate their differentiation into $CD4^+CD8^+$ cells. Consequently, the TCR repertoire expressed by early $CD4^+CD8^+$ thymocytes may already reflect the influence of intrathymic selection pressures.

REFERENCES AND NOTES

1. B. J. Fowlkes and D. M. Pardoll, *Adv. Immunol.* **44**, 207 (1989).
2. J. W. Kappler, N. Roehm, P. C. Marrack, *Cell* **49**, 273 (1987); B. J. Fowlkes, R. H. Schwartz, D. M. Pardoll, *Nature* **334**, 620 (1988).
3. H. S. Teh *et al.*, *Nature* **335**, 229 (1988).
4. H. von Boehmer, *Annu. Rev. Immunol.* **8**, 531 (1990).
5. W. Swat, L. Ignatowicz, H. von Boehmer, P. Kisielow, *Nature* **351**, 150 (1991).
6. W. C. Sha *et al.*, *ibid.* **336**, 73 (1988).
7. H. Pircher, K. Bürki, R. Lang, H. Hengartner, R. M. Zinkernagel, *ibid.* **342**, 559 (1989).
8. L. J. Berg, B. Fazekas de St. Groth, A. M. Pullen, M. M. Davis, *ibid.* **340**, 559 (1989); L. J. Berg *et al.*, *Cell* **58**, 1035 (1989); K. M. Murphy, A. B. Heimberger, D. Y. Loh, *Science* **250**, 1720 (1990); N. J. Vasquez, J. Kaye, S. M. Hedrick, *J. Exp. Med.* **175**, 1307 (1992).
9. D. J. Paterson and A. F. Williams, *J. Exp. Med.* **166**, 1603 (1987); H. R. MacDonald, R. C. Budd, R. C. Howe, *Eur. J. Immunol.* **18**, 519 (1988); K. Shortman, A. Wilson, M. Egerton, M. Pearse, R. Scollay, *Cell. Immunol.* **113**, 462 (1988).
10. T. Hunig, *Eur. J. Immunol.* **18**, 2089 (1988).
11. J. Nikolic-Zugic and M. W. Moore, *ibid.* **19**, 1957 (1989); H. T. Petrie *et al.*, *J. Exp. Med.* **172**, 1583 (1990).
12. Y. Takahama and A. Singer, unpublished results.
13. C. Benoist and D. Mathis, *Cell* **58**, 1027 (1989); H. R. MacDonald and R. K. Lees, *Nature* **343**, 642 (1990); L. A. Jones, L. T. Chin, D. L. Longo, A. M. Kruisbeek, *Science* **250**, 1726 (1990); B. Rocha and H. von Boehmer, *ibid.* **251**, 1225 (1991).
14. Tg-TCRαβ mice express the anti-male TCR and were originally developed by von Boehmer and colleagues (*4*). The *H-2*^{b} and *H-2*^{d} Tg-TCRαβ fetuses were obtained from C57BL/6 and BALB/c females, respectively, impregnated by a homozygous Tg-TCRαβ male mouse. Thymocytes from day 19 fetal mice were treated with RL172 MAb to CD4 [R. Ceredig, J. W. Lowenthal, M. Nabholz, H. R. MacDonald, *Nature* **314**, 98 (1985)] plus C and then separated by lympholyte-M (Cederlane Laboratories, Hornby, Ontario, Canada) centrifugation. These $CD4^-$ cells were further stained with MAb to CD8 (53-6-72; Becton-Dickinson, San Jose, CA) and sorted into $CD8^+$ ($CD4^-CD8^+$) and $CD8^-$ ($CD4^-CD8^-$) cells by a FACStar Plus cell sorter (Becton-Dickinson). Cells were cultured at 0.5 × 10^6 to 2 × 10^6 cells per milliliter in 24-well Costar plates in RPMI-1640 medium supplemented with 10% fetal bovine serum and 5 × 10^{-5} M 2-mercaptoethanol at 37°C in a humidified atmosphere with 5% CO_2. Cultured cells were stained with MAb to CD4 conjugated to FITC (Rm4-5; Pharmingen, San Diego, CA) and MAb to CD8 (53-6-72) conjugated to biotin and then with Texas red linked to avidin. The two MAbs to CD4, RL172 and Rm4-5, bind to different CD4 epitopes and do not compete with one another. All staining was performed in the presence of unlabeled MAb to the Fc receptor to block Fc receptor–mediated binding.
15. MAb to the TCRβ (H57-597) [R. T. Kubo, W. Born, J. Kappler, P. Marrack, M. Pigeon, *J. Immunol.* **142**, 2736 (1989)] was digested with immobilized pepsin (Pierce, Rockford, IL), and the purity of the resulting $F(ab')_2$ fragment was ascertained by SDS–polyacrylamide gel electrophoresis. Immunoglobulin G (IgG) fraction of MAb to CD3ε (145-2C11) [O. Leo, M. Foo, D. H. Sachs, L. E. Samelson, J. A. Bluestone, *Proc. Natl. Acad. Sci. U.S.A.* **84**, 1374 (1987)] was also used (2C11-IgG).
16. T. Goodman and L. LeFrancois, *J. Exp. Med.* **170**, 1569 (1989).
17. Fluorescence units (FU) are median intensity of CD4 staining minus median intensity of control MAb Leu4 staining. We calculated median intensity by converting median log channel number to linear units with an empirically derived calibration curve for each logarithmic amplifier used. Percent inhibition of CD4 FU was calculated as 100 × (FU of cultured cells with medium alone − FU of experimental group)/(FU of cultured cells with medium alone − FU of uncultured precursor cells).
18. Total cellular RNA was prepared from the indicated cell populations, and equal amounts of RNA (5 μg) were denatured, separated by electrophoresis on agarose gels, and transferred to nylon membranes as described [T. Maniatis, E. F. Fritsch, J. Sambrook, *Molecular Cloning: A Laboratory Manual* (Cold Spring Harbor Laboratory, Cold Spring Harbor, NY 1982)]. Blots were hybridized with a 2.1-kb Eco RI fragment of CD4 cDNA [D. R. Littman and S. N. Gettner, *Nature* **325**, 453 (1987)] or 1.3-kb Pst I fragment of rat glyceraldehyde 3-phosphate dehydrogenase (GAPDH) cDNA [P. Fort *et al.*, *Nucleic Acids Res.* **13**, 1431 (1985)] that had been labeled with ^{32}P by the random primer method.
19. $CD4^-$ day 19 fetal thymocytes from pools of unsexed *H-2*^{b} Tg-TCRαβ mice were prepared, cultured, and stained (*14*). MAb with indicated specificity [50 μg/ml; either H57-597 (H57) for MAb to TCRβ or MR5-2 (Pharmingen) for MAb to $V_\beta 8$] was coated onto the culture wells. Plastic-adherent cells (APCs) were prepared from spleen cells of T cell–deficient B10-*nu/nu* mice (*5*). Where indicated, thymocytes (0.5 × 10^6 cells per milliliter) were cocultured with APCs (0.4 × 10^6 cells per milliliter) in 24-well Costar plates.
20. Fetal Tg-TCRαβ mice on day 19 of gestation were sexed according to their internal genital organs [K. Theiler, *The House Mouse: Atlas of Embryonic Development* (Springer-Verlag, New York, 1989)].
21. $CD4^-$ day 19 fetal thymocytes were stained with FITC-conjugated MAb to CD5 (53-7-3; Becton-Dickinson) and biotinylated MAb to CD8 and then TR-avidin was added. CD5 expression was analyzed on electronically $CD8^+$ gated cells. Where indicated, $CD4^-$ day 19 fetal B6 thymocytes were cultured for 12 hours with PMA (100 ng/ml; Sigma).

22. We thank H. von Boehmer and M. Steinmetz for making their TCR transgenic mouse strain available to the scientific community; B. J. Fowlkes for providing a homozygous transgenic male breeder mouse; M. Sheard for assistance in flow cytometry and cell sorting; M. Kuehn and L. Lowe for helping in the sex diagnosis of fetal mice; and J. A. Berzofsky, R. J. Hodes, and D. S. Singer for critically reading the manuscript.

5 June 1992; accepted 20 August 1992

Flow-Dependent Cytosolic Acidification of Vascular Endothelial Cells

Roy C. Ziegelstein, Linda Cheng, Maurizio C. Capogrossi*

Hemodynamic shear stress affects endothelial cell structure and function, but little is known about the signal transduction mechanisms involved in these processes. The effect of laminar shear stress on cytosolic pH (pH_i) was examined in rat aortic endothelial cells cultured in glass capillary tubes. Shear stress forces led to a rapid decrease in pH_i (maximal effect 0.09 pH unit at 13.4 dynes per square centimeter). Removal of specific ions or addition of exchange inhibitors suggests that in vascular endothelial cells shear stress forces activate both an alkali extruder, sodium ion–independent chloride-bicarbonate ion exchange, and an acid extruder, sodium-hydrogen ion exchange; the net effect in physiologic buffer with the bicarbonate ion is a decrease in pH_i.

Shear stress forces modulate several vascular endothelial cell functions (*1*), but the signal transduction mechanisms involved in these processes have not been fully elucidated. Because shear stress leads to enhanced phosphoinositide turnover (*2*) and membrane hyperpolarization (*3*), both of which may influence cytosolic pH (pH_i) regulation, pH_i could provide a signal transduction mechanism in response to changes in flow. In addition, shear stress–induced changes in cytoskeletal organization or in agonist availability to the cell membrane might affect pH_i (*4*). To test the hypothesis that shear stress forces affect endothelial pH_i, we examined the effect of laminar flow on endothelial cells from the rat aorta cultured in glass capillary tubes (*5*).

When endothelial cells in glass capillaries were exposed to a HCO_3^--buffered solution equilibrated with 5% CO_2, the increase in laminar shear stress forces (*6*) caused a rapid and reversible decrease in pH_i (*7*) (Fig. 1). The threshold for this effect was below 0.5 dyne cm^{-2}, and it saturated between 6.7 and 13.4 dyne cm^{-2} (Fig. 1A). In a HCO_3^- buffer, exposure to 13.4 dyne cm^{-2} for 2 to 5 min resulted in an intracellular acidification of 0.09 ± 0.01 pH units ($n = 79$; $P < 0.0001$). A similar

Laboratory of Cardiovascular Science, Gerontology Research Center, National Institute on Aging, National Institutes of Health, Baltimore, MD 21224, and Johns Hopkins University, Division of Cardiology, Baltimore, MD 21205.

*To whom correspondence should be addressed.

response was observed in human aortic endothelial cells. No intracellular acidification was observed in human skin fibroblasts or in rat intestinal epithelial IEC-6 cells exposed to shear stress forces of 13.4 dyne cm^{-2} (8). Flow-induced cytosolic acidification of endothelial cells could be maintained for at least 30 min at 13.4 dyne cm^{-2}, but, at sustained shear stresses of 2.7 dyne cm^{-2} or less, pH_i returned to unstressed values (Fig. 1C).

The Na^+/H^+ exchange affects pH_i in vascular endothelial cells (9). Another acid extruder, extracellular Na^+ (Na^+_o)-dependent Cl^-/HCO_3^- exchange, and two alkali extruders, Na^+_o-independent Cl^-/HCO_3^- exchange and electrogenic Na^+-HCO_3^- cotransport, have been identified in other cell types (*10, 11*).

Shear stress–induced cytosolic acidification in HCO_3^- solution could be due to activation of an alkali extruder, resulting in loss of HCO_3^- from the cell. This possibility was examined by preincubating endothelial cells for 1 hour with 4-acetamido-4′-isothiocyanato-stilbene-2,2′-disulfonic acid (SITS) (*12*), an irreversible anion-exchange inhibitor. Preincubation with SITS substantially diminished the shear stress–induced acidification (Fig. 2). Incomplete inhibition of HCO_3^- transport may account for the inability of SITS to abolish this effect altogether. When experiments were performed in the absence of HCO_3^- (*13*), shear stress caused a small increase rather than a de-

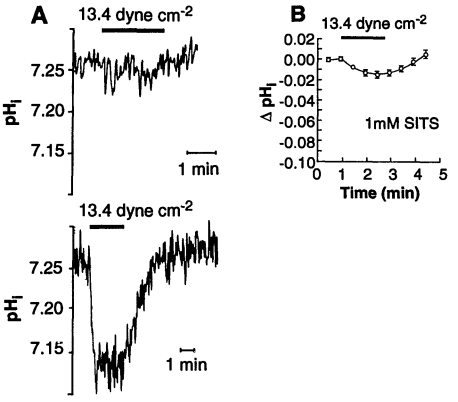

Fig. 2. Shear stress–induced cytosolic acidification in HCO_3^-/CO_2 buffer was blunted by preincubation for 1 hour with the irreversible anion-exchange inhibitor SITS (1 mM). (**A**) Representative tracings of the effect of shear stress forces at 13.4 dyne cm^{-2} on pH_i of control (lower trace) and SITS-treated (upper trace) endothelial cells. (**B**) Average effect of shear stress forces at 13.4 dyne cm^{-2} in SITS-treated endothelial cells; ΔpH_i was -0.01 ± 0.00 (n = 21). Endothelial cells that had not been exposed to SITS responded to similar shear stress by a ΔpH_i of -0.09 ± 0.01 (n = 79).

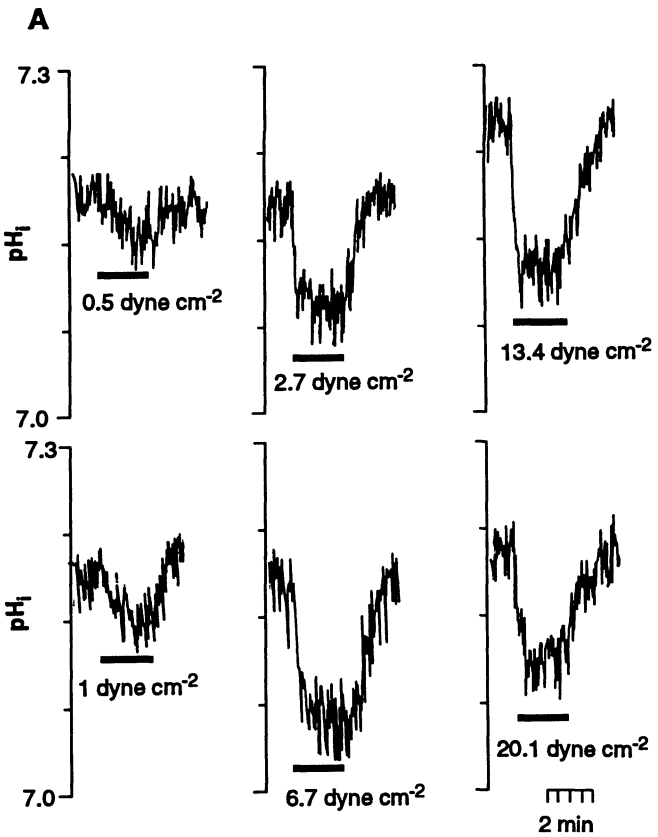

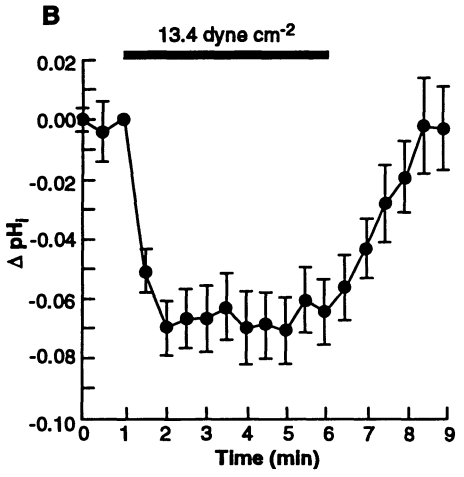

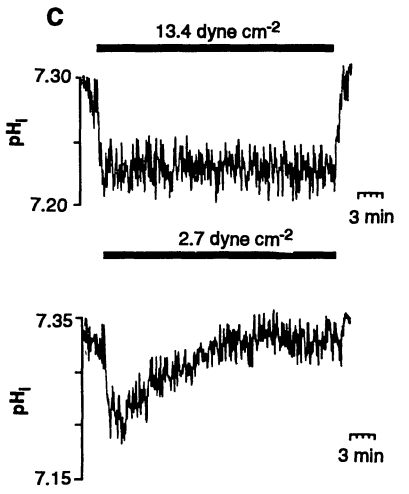

Fig. 1. Effect of shear stress forces on pH_i of vascular endothelial cells in a HCO_3^--buffered solution. (**A**) Changes in pH_i induced by different flow rates in the same monolayer of endothelial cells. (**B**) Average results on the effect of flow-induced shear stress for 5 min in HCO_3^-/CO_2 buffered saline. The average change in pH_i is plotted as a function of time in endothelial monolayers exposed to shear stress of 13.4 dyne cm^{-2} (n = 12). (**C**) Shear stress–induced cytosolic acidification was sustained for 30 min at 13.4 dyne cm^{-2} (upper tracing). In contrast pH_i spontaneously recovered over this time at 2.7 dyne cm^{-2} (lower tracing).

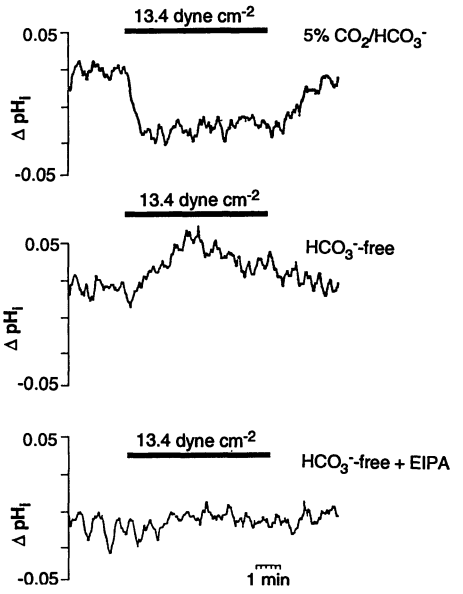

Fig. 3. Effect of flow-induced shear stress (13.4 dyne cm^{-2}) on one endothelial monolayer in HCO_3^-/CO_2 buffer or HCO_3^--free, Hepes-buffered saline, with and without EIPA. Flow-induced shear stress decreased pH_i in HCO_3^-/CO_2 buffer (upper tracing). In HCO_3^--free solution (middle tracing), shear stress forces caused a small increase in pH_i ($+0.02 \pm 0.00$ pH units; n = 9; $P < 0.002$) that showed partial recovery over a 6-min period. Cytosolic alkalinization in bicarbonate-free buffer was due to activation of Na^+/H^+ exchange, as it was inhibited by 10 μM EIPA (lower tracing).

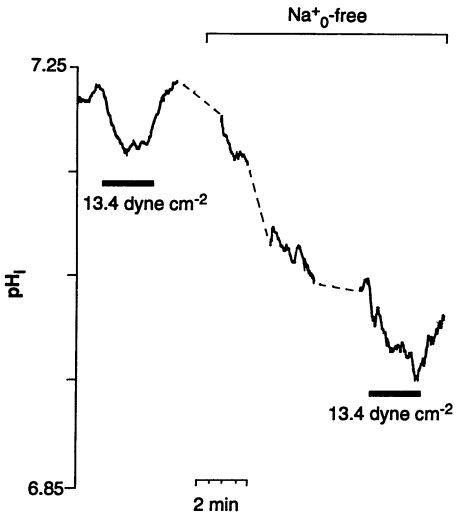

Fig. 4. Effect of flow-induced shear stress in a monolayer of endothelial cells exposed to HCO_3^-/CO_2 buffers with and without Na^+_o. When Na^+_o was fully replaced by tetramethylammonium (TMA) and choline, there was a rapid decrease in pH_i, but flow-dependent acidification was unaffected. In Na^+_o-free bicarbonate buffer, shear stress (13.4 dyne cm^{-2}) decreased pH_i from 7.06 ± 0.04 to 6.99 ± 0.03 (n = 5), a result similar to that in the presence of Na^+_o.

crease in pH_i (Fig. 3). Under these conditions, which inactivate HCO_3^- transporters, cytosolic alkalinization was abolished by ethylisopropylamilozide (EIPA) (*14*), a Na^+/H^+ exchange blocker (Fig. 3).

Of the various pH_i regulating mechanisms noted above only Na^+_o-independent Cl^-/HCO_3^- exchange does not rely on Na^+ transport for its function. To further distinguish among the ion transporters, we removed buffer Na^+ before shear stress exposure. When Na^+_o was completely replaced by choline and tetramethylammonium in a HCO_3^--buffered solution, pH_i decreased from 7.26 ± 0.04 to 7.06 ± 0.04 (n = 5). This suggests that under baseline conditions endothelial cells continuously extrude protons through Na^+_o-dependent mechanisms. Alternatively, the increase in Ca_i^{2+} that occurs when Na^+_o is removed (*15*) may decrease pH_i (*16*). Nevertheless, shear stress–induced cytosolic acidification at this new basal pH_i was not affected by Na^+_o removal (Fig. 4). This result in conjunction with that of anion exchange inhibition indicates that the cellular response to shear stress forces in the presence of HCO_3^-, which results in a decrease in pH_i, is due to Na^+_o-independent HCO_3^- extrusion.

Thus, we show that Na^+_o-independent Cl^-/HCO_3^- exchange occurs in vascular endothelial cells and that this transport mechanism as well as Na^+/H^+ exchange are activated by laminar shear stress. Different mechanisms may account for this finding. Flow-induced activation of an outward K^+ current (*17*) may modulate pH_i through changes in membrane potential (*18*) and in the intracellular concentration of ions linked to H^+ or HCO_3^- membrane transport. Alternatively, shear stress activation of Cl^-/HCO_3^- and Na^+/H^+ exchange may help regulate endothelial cell volume (*19*), as laminar shear stress within the range examined in the present report stimulates fluid-phase endocytosis (*20*).

In some nonendothelial cell types, an increase in cytosolic Ca_i^{2+} leads to a decrease in pH_i (*16*). In endothelial cells loaded with a fluorescent Ca^{2+} indicator, we and others did not observe an effect of brief exposures to shear stress on Ca^{2+}_i (*21*).

Shear stress enhances phosphatidylinositol turnover in endothelial cells (*2*), a process that is expected to be associated with the production of 1,2-diacylglycerol (*22*), which causes translocation to the membrane of Ca^{2+}-activated, phospholipid-dependent protein kinase C (PKC) (*23*). There is indirect evidence that one effect of shear stress forces is to enhance PKC activity (*24*). Shear stress activation of Na^+/H^+ exchange may be a consequence of these events, as PKC is known to activate Na^+/H^+ exchange (*25*).

In conclusion, our results establish that shear stress forces modulate mechanisms that have opposing effects on pH_i of vascular endothelial cells. In a physiologic HCO_3^--buffered medium, alkali extrusion predominates over acid extrusion, the net effect being a decrease in pH_i. The functional role of cytosolic acidification in response to rapid increases in shear stress forces, as may occur at the branching points of large arteries, remains to be defined.

REFERENCES AND NOTES

1. J. B. Lansman, *Nature* **331**, 481 (1988); P. F. Davies *et al.*, *Proc. Natl. Acad. Sci. U.S.A.* **83**, 2114 (1986); G. M. Rubanyi, J. C. Romero, P. M. Vanhoutte, *Am. J. Physiol.* **250**, H1145 (1986); J. A. Frangos, S. G. Eskin, L. V. McIntire, C. L. Ives, *Science* **227**, 1477 (1985); P. F. Davies *et al.*, *J. Clin. Invest.* **73**, 1121 (1984).
2. M. U. Nollert, S. G. Eskin, L. V. McIntire, *Biochem. Biophys. Res. Commun.* **170**, 281 (1990).
3. S.-P. Olesen, D. E. Clapham, P. F. Davies, *Nature* **331**, 168 (1988); M. Nakache and H. E. Gaub, *Proc. Natl. Acad. Sci. U.S.A.* **85**, 1841 (1988).
4. D. Ingber *et al.*, *J. Cell Biol.* **110**, 1803 (1990); T. Kitazono, K. Takeshige, E. J. Cragoe, Jr., S. Minakami, *Biochem. Biophys. Res. Commun.* **152**, 1304 (1988).
5. Rat aortic endothelial cells were cultured by the primary explant technique [O. F. Cole, T-P. D. Fan, G. P. Lewis, *Cell Biol. Int. Rep.* **10**, 399 (1986)]. Cells were grown in culture to passage 3 to 5 in minimum essential medium with D-valine supplemented with 20% fetal calf serum, endothelial mitogen (100 μg ml^{-1}), penicillin (5 mg ml^{-1}), streptomycin (5 mg ml^{-1}), and neomycin (10 mg ml^{-1}) at 37°C in a humidified atmosphere of 95% air and 5% CO_2 We identified endothelial cells by demonstrating specific immunofluorescent staining for factor VIII–related antigen and by measuring angiotensin converting enzyme activity. After treatment with 0.25% trypsin and 0.5 mM EGTA, cells were plated in 1-mm^2 glass capillary tubes precoated with 1% gelatin and allowed to grow to confluence on one face of the tube for 24 to 48 hours.
6. We achieved steady laminar flow by internally perfusing the glass capillary with a nonpulsatile pump. Shear stress was calculated as described [S-P. Olesen, D. E. Clapham, P. F. Davies, *Nature* **331**, 168 (1988)] by the formula $\tau = 4\ \mu Q/\pi r^3$, where μ = fluid viscosity, Q = flow rate, and r = internal radius (half-width). To keep r constant (0.5 mm), only a small area of the monolayer in the center of the tube was examined. A flow rate of 0.3 to 12 ml min^{-1} produced shear stress forces between 0.5 and 20.1 dyne cm^{-2}. A HCO_3^--buffered solution was used of the following composition (in mM): 116.4 NaCl, 5.4 KCl, 1.6 $MgSO_4$, 26.2 $NaHCO_3$, 1.0 NaH_2PO_4, 5.6 D-glucose, and 1.5 $CaCl_2$ (23°C) continuously gassed with 95% O_2 and 5% CO_2 to keep pH at 7.38 ± 0.01.
7. To monitor pH_i, we loaded cells with the membrane-permeant ester derivative (AM form) of the fluorescent H^+–sensitive indicator carboxy-seminaphthorhodafluor-1 (SNARF-1) [J. E. Whitaker, R. P. Haugland, F. G. Prendergast, *Anal. Biochem.* **194**, 330 (1991); P. S. Blank *et al.*, *Am. J. Physiol.* **263**, H276 (1992)]. Intracellular pH was monitored on the stage of a modified inverted microscope (P. S. Blank *et al.*, *ibid.*). After excitation at 530 ± 5 nm, the ratio of SNARF-1 emission at 590 ± 5 nm/640 ± 5 nm was used as a measure of pH_i. An in vitro calibration was obtained at 23°C with SNARF-1–free acid solutions at known pH values, and an intracellular calibration was obtained at 23°C from SNARF-1–loaded endothelial monolayers exposed to 140 mM KCl solutions of varying pH containing 20 μM nigericin, 1 μM valinomycin, and 1 μM carbonyl cyanide-*p*-trifluoromethoxy-phenylhydrazine (FCCP). There was no significant noncytosolic compartmentalization of SNARF-1 fluorescence in rat aortic endothelial cells as determined with cell fractionation by marker enzymes and SNARF-1 fluorescence distribution.
8. R. C. Ziegelstein, L. Cheng, M. C. Capogrossi, unpublished observations. Cells were a gift from J. L. Kinsella.
9. N. Escobales *et al.*, *Am. J. Physiol.* **259**, C640 (1990); D. Ghigo *et al.*, *J. Biol. Chem.* **263**, 19437 (1988).
10. R. C. Thomas, *Nature* **337**, 601 (1989), S. Liu, D. Piwnica-Worms, M. Lieberman, *J. Gen. Physiol.* **96**, 1247 (1990), W. F. Boron and E. L. Boulpaep, *ibid.* **81**, 53 (1983).
11. A. W. Siebens and W. F. Boron, *Am. J. Physiol.* **256**, F342 (1989); *ibid.*, p. F354.
12. S. Liu, D. Piwnica-Worms, M. Lieberman, *J. Gen. Physiol.* **96**, 1247 (1990); A. W. Siebens and W. F. Boron, *Am. J. Physiol.* **256**, F354 (1989).
13. The HCO_3^--free buffer used was of the following composition (in mM): 137.0 NaCl, 5.0 KCl, 1.2 $MgSO_4$, 1.2 NaH_2PO_4, 10 Hepes, 16 D-glucose, 1.5 $CaCl_2$ (pH adjusted to 7.39, 23°C).
14. N. Escobales *et al.*, *Am. J. Physiol.* **259**, C640 (1990); D. Ghigo *et al.*, *J. Biol. Chem.* **263**, 19437 (1988).
15. M. C. Capogrossi and R. C. Ziegelstein, unpublished results.
16. R. D. Vaughan-Jones, W. J. Lederer, D. A. Eisner, *Nature* **301**, 522 (1983).
17. S.-P. Olesen, D. E. Clapham, P. F. Davies, *ibid.* **331**, 168 (1988); M. Nakache and H. E. Gaub, *Proc. Natl. Acad. Sci. U.S.A.* **85**, 1841 (1988); J. P Cooke *et al.*, *J. Clin. Invest.* **88**, 1663 (1991).
18. Changes in membrane potential influence pH_i (*11*).
19. S. Grinstein, S. Cohen, J. D. Goetz, A. Rothstein, *J. Cell Biol.* **101**, 269 (1985); D. Gleeson, J. G. Corasanti, J. L. Boyer, *Am. J. Physiol.* **258**, G299 (1990); E. K. Hoffmann and L. O. Simonsen, *Physiol. Rev.* **69**, 315 (1989).
20. P. F. Davies *et al.*, *J. Clin. Invest.* **73**, 1121 (1984).

21. R. C. Ziegelstein, L. Cheng, M. C. Capogrossi, unpublished results; M. Mo, S. G. Eskin, W. P. Schilling, *Am. J. Physiol.* **260**, H1698 (1991); R. O. Dull and P. F. Davies, *ibid.* **261**, H149 (1991).
22. M. J. Berridge and R. F. Irvine, *Nature* **341**, 197 (1989).
23. M. Castagna *et al.*, *J. Biol. Chem.* **257**, 7847 (1982).
24. H.-J. Hsieh, N-Q. Li, J. A. Frangos, *J. Cell. Physiol.* **150**, 552 (1992).
25. S. Grinstein, S. Cohen, J. D. Goetz, A. Rothstein, *J. Cell Biol.* **101**, 269 (1985); W. J. Moolenar, L. G. J. Tertoolen, S. W. Delaat, *Nature* **312**, 371 (1984).

20 May 1992; accepted 4 August 1992

Role of Transmembrane Domain Interactions in the Assembly of Class II MHC Molecules

Pierre Cosson and Juan S. Bonifacino*

Evidence is presented that suggests a role for transmembrane domain interactions in the assembly of class II major histocompatibility complex (MHC) molecules. Mutations in the transmembrane domains of the class II MHC α or β chains resulted in proteins that did not generate complexes recognized by conformation-dependent antibodies and that were largely retained in the endoplasmic reticulum. Insertion of the α and β transmembrane domains into other proteins allowed the chimeric proteins to assemble, suggesting a direct interaction of the α and β transmembrane domains. The interactions were mediated by a structural motif involving several glycine residues on the same face of a putative α helix.

Class II molecules of the MHC are membrane-bound glycoprotein complexes expressed primarily in cells of the immune system, where the class II molecules function to present antigenic peptides to T lymphocytes. Class II molecules are composed of two polymorphic transmembrane subunits, α and β, that associate to form a noncovalent heterodimer (*1*). Both chains are type I integral membrane proteins, each consisting of two NH_2-terminal extracellular domains, a single membrane-spanning sequence, and a short COOH-terminal cytoplasmic tail (*1*). Assembly of the heterodimer occurs in the endoplasmic reticulum (ER), where the heterodimer associates with a type II integral membrane protein known as the invariant (Ii) chain (*2*, *3*). After assembly, αβIi complexes are transported through the Golgi system and into a prelysosomal compartment, where the Ii chain is proteolytically degraded (*2*, *3*). At this location, the αβ dimers bind antigenic peptides; the dimers are then delivered to the cell surface (*3*). The high degree of conservation of the transmembrane domains of class II MHC α and β gene products among various haplotypes and animal species (Fig. 1A) has suggested an essential role for these sequences (*1*, *4*). Because of the known function of transmembrane interactions in the assembly of other multiprotein complexes, such as in the assembly of the T cell antigen receptor (*5*, *6*) and Fc receptors (*7*), we decided to examine whether the membrane-spanning sequences were required for efficient assembly of newly synthesized class II MHC molecules.

Normal or mutagenized α and β chains of the I-A^k haplotype (*8*) were expressed in COS-1 cells (*9*). Transfected cells were metabolically labeled for 15 min and class II chains immunoprecipitated (*9*) with conformation-independent or -dependent antibodies (Abs) (*10*) (Fig. 2). Coexpression of α and β chains resulted in coprecipitation of both chains by conformation-independent Abs to the β or α chains (Fig. 2A) or by conformation-dependent Abs that require correct pairing of α and β subunits for reactivity (Fig. 2B). Insertion of a Bgl II site in the α and β cDNAs near the boundary between sequences encoding the extracellular and transmembrane domains resulted in replacement of three codons in both α and β (*8*) but had no effect on association (Fig. 2). We used this restriction site in order to replace the transmembrane domains of α and β by the transmembrane domain of the α chain of the interleukin-2 receptor (the Tac antigen) (*11*). The resulting αTα and βTβ chimeras associated, as assessed by coprecipitation with conformation-independent Abs (Fig. 2A). However, conformational epitopes found in normal class II MHC complexes were not generated (Fig. 2B), suggesting that the transmembrane domains of the α and β chains are required for correct assembly of αβ heterodimers. The nature of the chimeric protein species coprecipitated with conformation-independent but not conformation-dependent Abs is unclear. One possibility is that they represent complexes that are improperly assembled or that have an abnormal conformation. An alternative explanation is that the apparent association of the chimeric proteins does not reflect the formation of specific αβ dimers but rather the aggregation of unassembled α and β species with each other or with other intracellular proteins.

The subcellular localization of the normal and chimeric protein species was analyzed by immunofluorescence microscopy with a conformation-independent Ab to the β chain. These studies revealed that

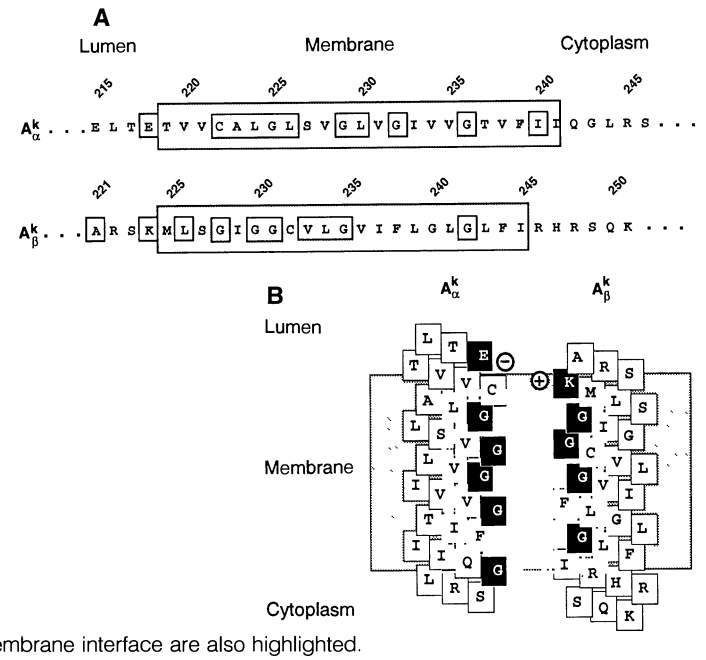

Fig. 1. (**A**) Sequences of transmembrane domains and adjacent regions of class II MHC chains of the I-A^k haplotype (*22*). Open boxes denote residues that are identical in >95% of all class II MHC chains examined [56 α and 124 β chain sequences (*24*)]. Amino acids are numbered from the initiator methionine of the normal A^k_α (*20*) and A^k_β (*21*) precursors. (**B**) Two-dimensional representations of I-A^k transmembrane domains, assuming an α-helical configuration (*13*). Conserved Gly residues on one face of the potential α helices are indicated by black boxes. Residues with charged side chains near the lumen-membrane interface are also highlighted.

Cell Biology and Metabolism Branch, National Institute of Child Health and Human Development, National Institutes of Health, Bethesda, MD 20892.

*To whom correspondence should be addressed.